Universidad Zaragoza
1542

Master's Degree in Nanostructured Materials for Nanotechnology Applications

Functionalization of Gold Nanoparticles for Cell Transfection

Author

Elena Lantero Escolar

Directors

Jesús Martínez de la Fuente

Yulán Hernández García

Universidad de Zaragoza – February 2015

Abstract

This report focuses on gold nanoparticle functionalization and checks their capability to transfect cells with a DNA plasmid, so the possibilities of the gold nanoparticles as vehicles for gene therapy can be explored. The nanoparticles were covered with a short polymer as stabilizer and, by the formation of an amide bound, different molecules of interest were conjugated to interact with a plasmid. Cell viability in presence of those functionalized nanoparticles was checked, and, finally, a transfection assay was performed. Transfected cells produced EGFP (Enhanced Green Fluorescent Protein), so they could be identified with fluorescence microscopy. Though some cells were transfected, the amount is really low, so more optimizations of the functionalization would be required to improve the process efficiency.

Resumen

Con intención de explorar las posibilidades de las nanopartículas de oro como vehículos para terapia génica, este trabajo se centra en su funcionalización y en comprobar su capacidad para transfectar células con un plásmido de ADN. En la funcionalización se han recubierto las nanopartículas con un polímero de cadena corta como estabilizante, y a éste, mediante formación de grupos amina, se le han conjugado distintas moléculas de interés que puedan interactuar con un plásmido. También se ha comprobado la viabilidad de células Vero en presencia de las nanopartículas funcionalizadas, y por último se ha realizado un ensayo de transfección. Las células transfectadas producían EGFP (Enhanced Green Fluorescent Protein) para ser identificadas por microscopía de fluorescencia. Aunque algunas células sí que se transfectaron en el proceso, la cantidad es muy baja, por lo que se requerirían optimizaciones de la funcionalización para incrementar la eficiencia del proceso.

Contents

Acronyms / Abbreviations

NPs	Nanoparticles
AuNPs	Gold Nanoparticles
TEM	Transmission Electron Microscopy
PEG-COOH	α-tio-ω-(propionic acid)octa(ethylene glycol)
EDC	*N*-(3-Dimethylaminopropyl)-*N'*-ethylcarbodiimide hydrochlorhide
S-NHS	*N*-hydroxysulfosuccinimide sodium salt
TEPA	Tetraethylenepentamine
EDA	Ethylenediamine dihydrochloride
PEI	Poly(ethyleneimine)
$R'R_3N^+$	(2-aminoethyl)-trimethylammonium hydrochloride
TAMRA	Tetramethylrhodamine 5-(and -6)-carboxamide cadaverine
MTT	3-(4,5-dimethylthiazol-2-yl)-2,5-diphenyltetrazolium bromide

1. Introduction

1.1. Nanomaterials and Nanotechnology

The Greek word *nanos* –from which comes the prefix 'nano'- means dwarf. In science, 'nano' is used to indicate a factor of 10^{-9} or one billionth. Despite the existence of different definitions of nanomaterials, according to the European Commission of Enviroment, these objects have at least one dimension between 1 and 100 nanometers long[1]. At the same time these new materials can be natural, incidental or manufactured depending on their synthesis process and from now on, this work will be focused on the manufactured ones because of being the main interest of the nanotechnology.

The progression towards downsizing to reach tighter results developed by the conjugation of many different sciences and their techniques (from chemistry, materials science and physics to pharmacology, genetic engineering and so on) has given as result the nanotechnology. That is why it is described as an interdisciplinary field, because the different sciences that pursuit the control of processes and products in the nanoscale and their applications can be considered part of the nanotechnology. Nanotechnology's main goal consists of controlling architecture, composition and physical properties with atomic resolution[2].

Just to give an idea of the increasing importance of this new field of investigation and development, in Spain 342 research groups and companies are dedicated to it. Approximately 2500 researchers, technicians, etc. work in these groups[3].

Nanotechnologists highlight the new characteristics observed in these new materials. Due to their size, nanomaterials present novel physical, chemical and biological properties, that make them suitable for a wide range of applications.[2]

Any material that can be built, resized, reordered or patterned with at least one dimension between 1 and 100 nm could be considered a nanomaterial. Nanoparticles (NPs) are those materials which have all their three dimensions in that range of size. There are two ways of obtaining NPs, depending on which material is used as precursor: when bulk material (like gold slices) is divided into really small fragments as nanoparticles, it is called a "**Top-down**" approach (i.e.: laser ablation of gold plates can provide gold nanoparticles[4]); when compounds such as gold salts are used, gold ions are reduced and

then form small seeds or nucleus, that will grow and form the nanoparticles, that is a "**Bottom-up**" approach (examples are explained in section 1.3.).

Among all of the materials that can be used to obtain NPs, because of their extraordinary optical properties and their relatively easy functionalization, gold nanoparticles have been chosen for this project.

1.2. Properties of Gold Nanoparticles and their applications

Gold nanoparticles (AuNPs) show some properties that vary depending on the size, the shape, the distance between particles, the nature of the stabilizing coating, etc[5]. Some reviews introduce the importance of the quantum size effect and the relevance of quantum-mechanical rules in these metallic nanoparticles. The tunnel effect and similar phenomena have great practical impact on the development of different systems such as transistors, switches, biosensors or catalysis, among others.[5,6]

As it has been widely described, AuNPs are biocompatible and non-toxic[7], which make them suitable for biomedical applications. Their high atomic weight allows them to scatter X-ray, so they could be applied as image contrast in radiographies[8], for example.

The exceptional optical properties of AuNPs have great interest for their characterization and applications. They have 'surface plasmon resonance' bands, a phenomenon produced by the electronic charge oscillations localized in the nanoparticle surface, which increase the field amplitude when irradiated at the resonance wavelength. This phenomenon was explained mathematically by Mie[9], and it is also present in other metallic nanoparticles. For gold, silver and copper, the resonance wavelength can be found in the visible range (depending on size and shape) and for this reason it can be observed by UV-Vis spectrophotometry. This technique provides the UV-visible absorbance spectrum of AuNPs, which have a peak with the maximum at the resonance wavelength. Peak shape and position (and therefore the resonance wavelength) is related with the particle size and shape, and distance between particles[10].

The plasmon band is influenced by particle shape, medium dielectric constant and temperature[6]. Figure 1D illustrates the correlation between different shapes and their absorption spectra. Stabilizers and ligands closely attached to the surface of AuNPs,

change the refractive index, inducing also a deviation in the absorption band[6]. These changes and its sensitivity has been exploited to build simple colorimetric sensors for biological samples[11].

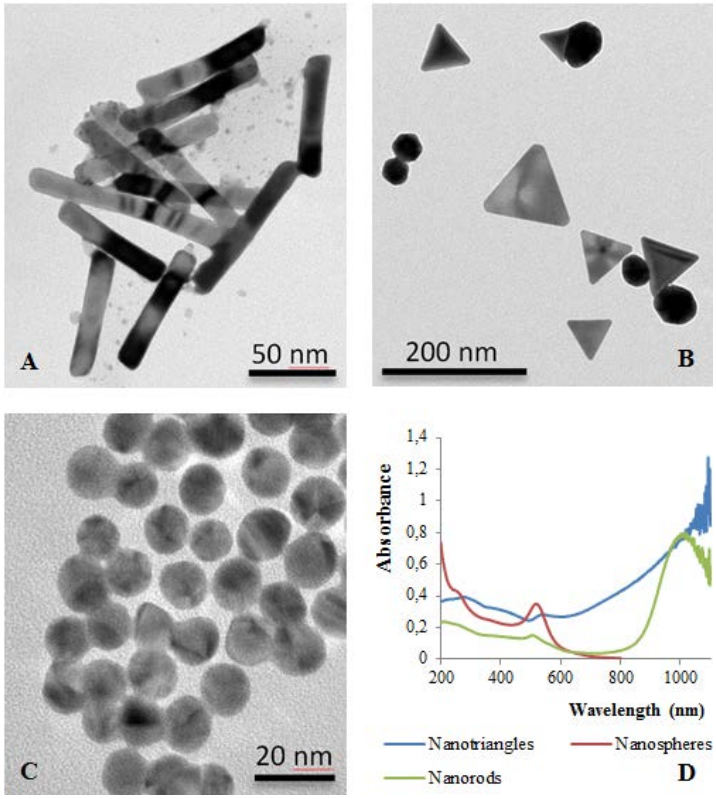

Figure 1: Transmission Electron Microscope (TEM) Photographies from differently shaped nanoparticles and their absorvance spectra. In (A) there are nanorods, which have their bigger peak of absorption at 1000 nm approximately. (B) are nanotriangles, with a peak around 1100 nm. (C) shows small nanospheres, which have a peak in their spectrum at 520 nm. (D) correspond to absorption spectra of the tree types of AuNPs. Images and spectra from nanorods and nanotriangles were taken by Álvaro Artiga.

Beside this phenomenon, AuNPs can also induce a quenching effect on fluorophores and a surface-enhanced Raman scattering which allows an enhanced detection of small quantities of molecules attached to them. These properties have also been applied to design sensors[8].

In addition to all these possibilities, the photothermal properties of AuNPs may be used for many applications. When nanoparticles get excited in the plasmon band wavelength, the oscillation of the electron cloud and its energy can be released in form of heat, increasing the temperature of the surrounding medium. This effect has been applied in different applications such as photothermal therapy, sensors sensitive to changes in the temperature and in drug delivery inducing the release of molecules attached to the surface of the nanoparticle.[8]

For all these applications, the versatile synthesis and functionalization of AuNPs provides an important advantage, as it allows the possibility of modifying the gold surface with a wide range of molecules or coatings, which broadens their possible uses.

1.3. Synthesis and functionalization of Gold Nanoparticles

AuNPs have been used since ancient times in glass, ceramics and paintings, although there was no conscience of the size, structure or components that such materials had. In 1857, Faraday was pioneer in reporting the synthesis of AuNPs –made from the reduction of a gold salt using phosphor– and studying their properties when dried into thin films[12]. In 1861, Graham *et al*. described these nanoparticles in solution as colloids, from the French, *colle*, that means 'mixture of dry ingredients in a liquid'[13].

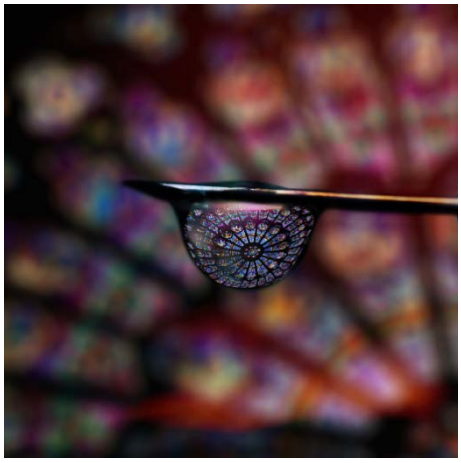

Figure 2: To obtain different colors in glasses, they were stained with different nanoparticle coloids since middle age. Photography by Marta Palacio.

During the twentieth century, many approaches were tested to produce AuNPs, obtaining nanoparticles of different shapes and sizes and capped with different stabilizing agents.

The most common and reproducible techniques for the synthesis of AuNPs are "bottom-up" approaches such as Faraday's experiments and the examples described below.

In many studies sodium borohydride ($NaBH_4$) has been used as reductor agent of gold salts in aqueous media, in the presence of other molecules that act as stabilizing agents[14,15]. In some others, molecules such as polysaccharides (i.e. chitosan) have been used as both reducing and stabilizing agents[16].

AuNPs have been also synthetized in organic media by Schmid *et al.* (in benzene, using Chloro(triphenylphosphine)gold(I) as precursor and diborane as reducer)[17] and using a two-phase system (in water-toluene and using dodecanethiol as reducer of $HAuCl_4$) in the so-called Brust-Schiffrin method[18]. The disadvantage of these approaches is that nanoparticles need to be transferred to water to be used in biomedical applications[19].

Among all the techniques, one of the most used is the Turkevich method, in which a **chloroauric salt is reduced and stabilized using sodium citrate** in aqueous solution[20]. The size distribution obtained by this method was improved by Frens[21], allowing the selection of the size of the final product. Spherical nanoparticles are obtained, with a narrow size distribution and high reproducibility. Beside this, the AuNPs are dispersed

Figure 3: Representation of a gold nanoparticle stabilized by citrate molecules. In Turkevich method, citrate acts as both reductor and stabilizing agent.

in aqueous media, which allows their use in biological applications without the phase transference to aqueous medium required by other methods[17–19].

Some works[21,22] point out the importance of the citrate concentration and how it is related to gold particle size: a high citrate concentration stabilizes small particles, whereas a smaller citrate concentration does not completely cover those small AuNPs, that aggregate and form larger particles. That is why, when controlling the citrate concentration, it is possible to obtain AuNPs of a desired size in a range from 9 to 120 nm[22].

Because of their ionic nature, interactions between citrate molecules and the gold core are weak, so stronger stabilizers are needed for the nanoparticles to remain stable in biological conditions (high concentration of salts, pH around 7.4, etc.). Interaction with the gold surface can be established through adsorption[23], quasi-covalent and covalent interactions.

The **interaction formed between sulfur atoms and the gold surface** has been widely studied[24]. It is a strong bond, and has already been used for attaching many kinds of molecules to the AuNPs surface[15,19,25]. This bonding has been chosen in the present work for its strength and stability.

Besides the direct bonding with thiol groups, **molecules can be conjugated indirectly**, by using the stabilizer already attached to the gold surface and/or linkers, as far as they have the appropriate groups to interact between them. For example, molecules have been attached to the stabilizer using click chemistry[26] among other reactions. Moreover, it is possible to grow polymer chains directly over the AuNPs surface when the stabilizing molecule acts as initiator of the polymerization, obtaining nanoparticles coated with a polymer. The polymeric growth occurs spontaneously after adding the molecules that become polymeric subunits after the reaction[27].

Another technique to conjugate molecules is forming amide groups from the coupling reaction between carboxyl and amino groups, process known to be favored in the presence of carbodiimide. The reaction does not occur spontaneously, so carbodiimide compounds are used to ‘activate’ the carboxyl group. N-(3-Dimethylaminopropyl)-N’-ethylcarbodiimide (EDC) has been extensively used for conjugating and modifying bi-

omolecules[28,29]. This molecule forms an intermediate with the carboxyl group (*O*-acylisourea) more reactive in presence of amine groups, inducing the formation of a covalent amide bonding between both groups. This process has some limitations, the pH range in which it can be performed is difficult to set, because EDC is stable at neutral and higher pH regions, but the range of pH in which the *O*-acylisourea is formed is 3.5-4.5, and the amine groups require a pH above or near their pKa for promoting amide formation[30]. In addition, the intermediate is susceptible of hydrolyzing in aqueous media[31], or inactivation by intramolecular transference[32].

In order to stabilize the intermediate, compounds such as *N*-hydroxysuccinimide (NHS) have been simultaneously added with the EDC[32]. This molecule reacts with the intermediate, producing a succinimidyl ester, more stable and more reactive towards amine groups. The reaction yield has been notoriously increased when NHS is added[33].

NHS derivatives, like *N*-hydroxysulfosuccinimide (S-NHS) are used for the same pourpose[31]. EDC and S-NHS have been used in the present project for conjugating different molecules to the nanoparticles.

The functionalization of AuNPs varies depending on the final application. For biomedical purposes, it is convenient having fluorophores or other labels so they can be followed inside a cell or organism. They may also present molecules that favor cell targeting, cell uptake and internalization –like carbohydrates, peptides or antibodies– so they can get inside cells to accomplish their function. Many molecules of interest for the final application –like drugs, DNA, proteins, enzymes, etc.– can also be attached to the nanoparticle surface through the described interactions.

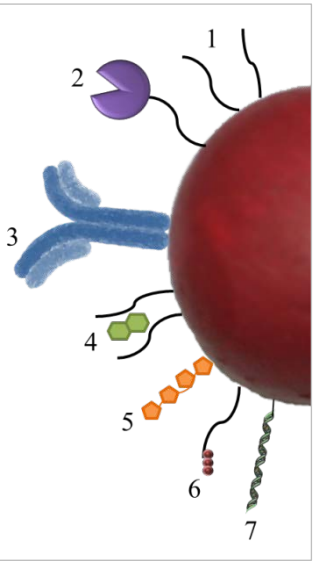

Figure 4: Scheme of different molecules that can be attached to AuNPs, such as: 1 stabilizer ligands, 2 enzymes and proteins, 3 antibodies, 4 hydrophobic drugs, 5 carbohydrates, 6 fluorophores and 7 nucleic acids as DNA. All of them can be attached directly to the gold surface or by interaction with the stabilizing coating, depending on the design and application.

1.4. Applications of AuNPs in delivery

AuNPs have some advantages when used in delivery applications compared with classical delivery systems such as liposomes or polymeric capsules, mainly related with their optical and photothermal properties, but also a lower toxicity, essential for working with biological systems. Some other characteristics exploited for delivery are shared among different kinds of vehicles, such as: appropriate size to enter into cells, high surface/volume ratio to load a great amount of molecules, stability in solution, variety of functionalizations and biocompatibility.

AuNPs can be functionalized with the molecules of interest through many approaches, varying the strength of the attachment between both species[34]**.** Many techniques involve **surface interaction**, such as those drugs with thiols or free amines that **binds directly to the AuNP surface**, or molecules **conjugated to the stabilizer** attached either by **covalent or ionic interaction**.

In a previous review[8], AuNPs application in delivery were classified depending on the loaded molecule; thus AuNPs could be used as vehicles for **gene therapy** or for **drug targeting**.

Gene therapy vehicles (also known as vectors) carry nucleic acids, either DNA or RNA into cells, allowing the expression of the gene carried (in case that it is not expressed or has undergone mutation in the target cell) or inhibiting the expression of one or more genes, providing a treatment for a disease or condition originated genetically or with genic consequences, such as cancer or some immunodeficiencies. The mechanism is briefly explained in figure 5.

The usual vehicles in gene therapy are modified virus[35,36], which already have the mechanisms to induce gene expression of the nucleic acids that they carry. Their disadvantages are: the immune response that they produce (that limits their reaching to the target cells), and poor control of the infection[35]. Some other strategies have been developed[37,38], involving nanomaterials as a promising tool to deliver nucleic acids. AuNPs have some advantages: they induce a low immune response and their flexibility of functionalization allows a better targeting and a higher control of loading and release of nucleic acids. Also, combinations of carriers –such as adenoviruses attached to AuNPs– have been tested so advantages of both systems can be exploited[39].

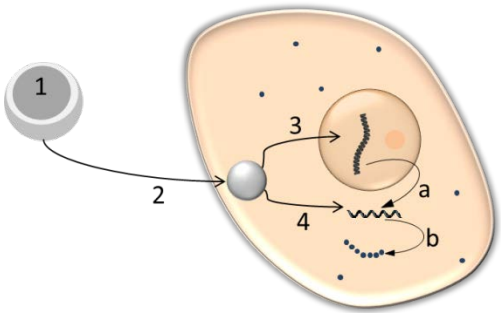

Figure 5: Schematic representation of a cell and the gene therapy process. There are many types of vehicles (1) such as viruses and NPs, that need to enter into cells (2) and release the nucleic acid. If it is DNA (3) has to enter into the nucleous and will be transcripted (a) and translated (b) into a protein. If it is RNA, it interferes with the translation process, avoiding one or more genes to be expressed.

When gene therapy is performed with DNA and non-virus vehicles, transfection is needed to be successful. Transfection is the process of introducing and expressing external genes in a cell. The usual molecule used in transfection is a DNA plasmid: a circular molecule of DNA that contains the gene of interest and able to replicate independently. The sequence for replication in bacteria is used for obtaining plasmid copies inside of bacteria cells, as, while these replicate, big amounts of plasmid can be obtained (one copy at least for each bacterium that contains it). To allow the expression in eukaryotic cells, the gene of interest needs to have appropriate sequences for transcription and translation, so a protein will be formed in the host cell.

This work proposal goes in the direction of obtaining an efficient delivery vector for carrying plasmids conjugated by ionic interaction. For this strategy, it is important to reach a compromise in the strength of the attachment, strong enough to avoid releasing the desired molecule before reaching the cell, but weak enough so it does not hinder its release once inside the cell.

Different molecules have been used here for the functionalization, by conjugating them to the outer stabilizing coating. All of them are positively, at least in physiological pH, so they can interact with DNA plasmids, which are polyanionic due to the phosphate groups present in their backbone.

Another function of cationic charges is inducing the disruption of endosomes membranes, leading to the DNA liberation inside the cell, through a process known as ‘proton sponge’. This has been studied when polycations such poly(ethyleneimine) (PEI) of high molecular weight are used for transfection[40]. PEI and DNA complexes are endocyted by the cell, provoking the entrance of lots of protons inside the endosome, captured by PEI, and inducing the uptake of chloride ions to equilibrate charges. The osmotic pressure ends disrupting the membrane and the DNA can be liberated in the cyto-

sol. As the AuNPs used in this work have cationic charges in their surface, they could induce a similar process but without the high cytotoxicity that high-molecular-weight PEI has.

The packaging produced from the interaction between AuNPs and plasmids can also protect DNA from lysosomal nucleases. This effect has been observed for polycation complexes with DNA[41], and may also be applied for cationic charged nanoparticles.

As final remarks, a DNA plasmid that codes for the reporter gene *Enhanced Green Fluorescent Protein* (EGFP) has been used in this project. This way, as the product of the expression of that gene is a fluorescent protein, the efficiency of these AuNPs as carriers for transfection could be evaluated directly by fluorescence microscopy.

2. Objetives

The present work pursues the following goals:

- Synthetize gold nanoparticles by the Turkevich method.
- Functionalize the nanoparticles with a polymer coating (stabilizer) and set the appropriate conditions to conjugate them to molecules with amine groups.
- Characterize those nanoparticles.
- Check interactions with a DNA plasmid and quantify plasmid/AuNP ratio.
- Evaluate the cell viability on a selected cell line (Vero) when treated with the different types of functionalized AuNPs, either with or without plasmids.
- Perform transfection assays into epithelial cells (Vero), to check if these AuNPs are suitable for DNA delivery.

3. Material and methods

All the reactants were purchased at Sigma Aldrich unless it is specified another company.

3.1. Synthesis of Gold Nanoparticles.

A solution of 80 mg of $HAuCl_4$ (Strem Chemicals) in 200 mL of milliQ water was prepared into a round-bottom flask (previously cleaned in aqua regia and oven-dried), and then heated and stirred in a bath under reflux. Once it started boiling, 5 mL of a 47.98 mg/mL sodium citrate solution were added, changing the solution color from pale yellow to black and in a few seconds it turned red. It was maintained for 30 minutes at boiling temperature, and then, removed from the bath. During the process it was wrapped in foil to avoid photodegradation.

3.2. Functionalization with PEG

The AuNPs were coated with the commercial chain α-tio-ω-(propionic acid)octa(ethylene glycol) (PEG-COOH, Iris Biotech).

For the first assays, differences in functionalization were checked with different quantities of PEG-COOH and following two different incubation processes. Different amounts of PEG-COOH (10-75 µL) from a stock solution of 1 mg/mL were added to a mixture of 10 pmol of AuNPs, 2.5 µL of SDS 11.1 %, and 12.5 µL of NaOH 2M and MilliQ water was added up to 1 mL. A group of samples were sonicated for 1 hour in a bath; followed by incubation and stirring overnight at room temperature. The other group was directly incubated overnight at room temperature without the sonication step.

After optimizing conditions, the reaction was scaled up functionalizing 500 pmol of AuNPs per batch. Two types of functionalization were chosen for this scaling up: those functionalized with 75 µg of PEG-COOH per 10 pmol of AuNPs with the protocol including a sonication step, and those functionalized with 25 µg of PEG-COOH per 10 pmol of AuNPs without sonication.

In all cases, three cycles of washing were performed by centrifuging at 14000 rpm at 4°C during 30 minutes, eliminating the supernatant and suspending in milliQ water.

The Ellman assay was performed as follows: in an ELISA microplate 218 µL of each sample were added into a well with 54.4 µL of TRIS buffer pH 8 and 27.6 µL of DNTB 2 mM in NaAc 50 mM. After 10 minutes, the absorbance was measured at 412 nm in a microplate reader.

3.3. Further functionalizations

The carboxyl groups of the PEG-COOH coating were activated to allow their attachment to amine groups of other molecules of interest. The activation was performed by mixing N-(3-Dimethylaminopropyl)-N'-ethylcarbodiimide hydroclorhydre (EDC) and N-hydroxysulfosuccinimide (S-NHS) in 500 µL of MES 0.1M pH 6. After 10 minutes of agitation, 20 pmol of nanoparticles and milliQ water (until reaching 1 mL of volume) were added, and the mixture was incubated and stirred for 20 minutes. After that, the excess of EDC and S-NHS was removed by centrifugation with Amicon-Ultra® 100KDa (Millipore) at 13400 rpm for 5 minutes and resuspended in 500 µL of milliQ water. Then, the conditions were as follow in each different assay.

- **Using (2-aminoethyl)-trimethylammonium hydrochloride ($R'R_3N^+$):**

After removing the excess of EDC and S-NHS, the activated nanoparticles were divided into two duplicates with 250 µL of MES 0.1M pH 6 each and the appropriate quantity of $R'R_3N^+$ from a 100 mg/mL solution was added. Samples were incubated for 2 hours at room temperature under agitation. Then, nanoparticles were washed 3 times by centrifugation at 14000 rpm at 4°C for 30 minutes, the supernatant was removed and they were resuspended in milliQ water.

To check the appropriate conditions for the activation, different amounts of EDC (0-40 µL) and S-NHS (0-80 µL), both from a 100 mg/mL solution, were used for the activation, while keeping constant the amount of $R'R_3N^+$ (20 µL of a solution 100 mg/mL).

To confirm the appropriate quantity of $R'R_3N^+$ to induce changes in the net charge of the particles, the activation was performed with 2.5 µL EDC and 5 µL S-NHS (both 100

mg/mL) and different amounts of $R'R_3N^+$ (0-40 µL from a 100 mg/mL solution) were added afterwards.

- **Using Tetraethylenepentamine (TEPA):**

In the first assay, performed to check the appropriate conditions, activation was done with 5 µL of EDC and 10 µL of S-NHS (both 100 mg/mL) in MES pH 6 50mM. After removing the excess of these compounds, nanoparticles were divided into duplicates and resuspended in different buffers: MES pH 6, NaP pH 7.5 and borate buffer pH 9; all of them 50 mM of final concentration. Then, 4 µL of a 1/100 solution of the commercial TEPA solution, with similar pH to the buffer, were added to each duplicate. Samples were incubated for 2 hours at room temperature under agitation. Then, they were washed 3 times by centrifugation at 14000 at 4°C for 30 minutes, the supernatant was removed and they were resuspended in milliQ water.

Further assays with TEPA were developed in borate buffer, with the convenient amount of TEPA from the 1/100 solution at a pH close to 9.

In order to check the appropriate conditions for the activation, different amounts of EDC (0-20 µL) and S-NHS (0-40 µL) -both from a 100 mg/mL solution- were used and 4 µL of the TEPA solution were added afterwards.

To check the appropriate quantity of TEPA needed, 5 and 10 µL of EDC and respectively 10 and 20 µL of S-NHS (from 100 mg/mL solution) were used for the activation, and different amounts of the TEPA solution (0-10 µL) were added. The incubation and washing steps were performed as described before.

- **Using Ethylenediamine dihydrochloride (EDA):**

The first experiment was performed using also different buffers, right after the activation with 5 µL of EDC and 10 µL of S-NHS (both 100 mg/mL). MES pH 6, NaP pH 7.5 and borate buffer pH 9, all of them 50 mM of final concentration, were used. After that, 7 µL of an EDA solution (1 mg/mL) were added, and the incubation and washing processes were developed as described before.

In further experiments, MES buffer was used during the whole functionalization. To check the activation conditions, different amounts of EDC (0-20 µL) and S-NHS (0-40 µL) -both from a 100 mg/mL solution- were used for that process, and 7 µL of an EDA solution (1 mg/mL) were added after removing the excess of activation compounds.

They were incubated for 2 hours and washed by centrifugation in the same conditions as in previous assays.

Finally, different quantities (0-15 µL) of EDA were used after activation with 10 µL EDC and 20 µL S-NHS solutions, following the same procedure for incubation and washing.

- **Using Poly(ethyleneimine) (PEI)**

In the first assay, activation carried out with 5 µL EDC and 10 µL S-NHS (both solutions of 100 mg/mL), and, after removing the excess, different buffers were used in the next step: MES pH 6, NaP pH 7.5 and borate buffer pH 9; all of them at a final concentration of 50 mM. Then, 12 µL of a 1/1000 solution from a 50% wt stock of PEI were added and the next steps followed the same process of incubation and washing as before.

The activation in next assays with PEI was also performed with 5 µL EDC and 10 µL S-NHS (both solutions of 100 mg/mL) and the convenient quantity of PEI (varying from 0 to 12 µL of a 1/10 solution) was added to each sample. The incubation and washing processes were developed as described before.

- **Using Tetramethylrhodamine 5-(and -6)-carboxamide cadaverine (TAMRA)**

TAMRA (Anaspec) is a fluorophore used for tagging the AuNPs. Its amine group allows coupling with EDC and S-NHS activated carboxyl group. It was conjugated simultaneously with the other molecules.

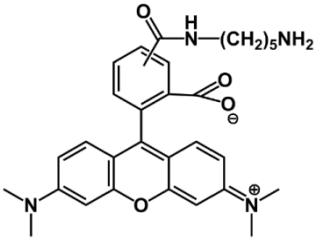

Figure 6: TAMRA's structure.

In order to set appropriate conditions for simultaneous bonding, activated nanoparticles and a control of non-activated AuNPs (non-sonicated Au@COOH) were incubated with TAMRA (0-6 µL of 1mg/mL solution per duplicate) in MES 50 mM pH 6 during different times (from 0 to 60 minutes) before adding 1.3 µL of $R'R_3N^+$ (100 mg/mL) per duplicate. Then the mixture was kept stirring for 2 hours and washed 5 times by centrifugation, taking supernatants and adding PBS-tween 0.1% (supernatants were kept for indirect quantification of TAMRA bonded). As 60 minutes were needed to obtain an important difference of TAMRA bonded to the nano-

particle before adding $R'R_3N^+$, next assay with sonicated Au@COOH was performed in that conditions.

To simultaneously conjugate either EDA or PEI to the nanoparticles, the same conditions were applied, using 15 µL of a 1 mg/mL EDA solution or 12 µL of a 1/100 of the PEI comercial solution per duplicate in each case. Assays with EDA were performed only with sonicated Au@COOH.

The conditions were different from the described above when bonding TAMRA and TEPA to the nanoparticles: incubating at pH 9 (in borate buffer 50 mM) with TAMRA induced the aggregation of the nanoparticles and TAMRA lost fluorescence. Best results were obtained when activated AuNPs were incubated with TAMRA in MES 50 mM pH 6 for 45 minutes, then washed by centrifugation and resuspended in borate buffer 50 mM pH 9, to end with the addition of 1µL of TEPA (1/100 dilution from commercial solution) per duplicate, and stirring during two hours before washing by centrifugation with PBS-tween 0.1% three times and with milliQ water two times.

TAMRA was indirectly quantified by diluting 1:2 in PBS-tween 0.1% the supernatants in a 96-well plate. In the same plate increasing quantities of TAMRA (from 0 to 1 µg) were prepared in PBS-tween 0.1% by duplicate to set a calibration curve. A plate reader Synergy HT (Biotek) provided amount of fluorescence when the sample was excited at 560 ± 40 nm. Emitted fluorescence was measured at 620 ± 40 nm. Correlation between fluorescence and TAMRA quantity was established and calculus and histograms were made in Microsoft excel.

3.4. Characterization

The nanoparticles were characterized using UV-Vis spectra, measured in a Varian Cary 50. This technique was also used for calculating the concentration of nanoparticle solutions, as the extinction coefficient of 14 nm spherical AuNPs at 450 nm is known to be $1.76 \cdot 10^8 \ \ M^{-1} \cdot cm^{-1}$.[42]

TEM images were taken with a Tecnai T20 (FEI) microscope, with a thermoionic gun and 200kV of acceleration voltage. The samples were highly diluted in water and a drop was placed over a carbon covered cupper grid (Electron Microscopy Sciences). About

100 NPs were measured, using Image J software (http://rsbweb.nih.gov/ij), and histograms were made with Microsoft Office Excel.

The electrophoretic mobility of the nanoparticles was analyzed by electrophoresis in gels with 0.8% of agarose (Lonza) in buffer TBE 0.5X (Tris-Borate-EDTA) at 90V for 30 minutes.

Hydrodynamic diameter was measured using dynamic light scattering (DLS) and AuNPs net charge by measuring Z potential. Samples were diluted up to 0.4 nM in milliQ water, previously filtered with filters of 0.2 µm pore. Finally pH was adjusted using NaOH 0.01 M and HCl 0.01M. Both techniques were performed in a Zetasizer nanoseries (Malvern Instruments) using the software provided with the equipment. For DLS, data analysis was made using gold refracting index (2.64 real part and 1.63 imaginary part) and number percentage values were used.

3.5. Plasmid obtention

The plasmid was extracted from the bacteria culture using NucleoBond® Xtra Midi kit (Macherey-Nagel), following its instructions. The concentration was calculated by absorbance measurements at 260 nm using a microplate reader and a µDrop™ Plate (Thermo Scientific).

3.6. Plasmid and nanoparticles incubation

Different quantities of pEGFP plasmid (0-1 pmol) were incubated with 0.2 pmol of nanoparticles, in a 40 µL solution, during 30 to 60 minutes. Then, the mixture was washed by centrifugation at 8000 rpm 45 minutes at 4°C two times, resuspending with milliQ water. Plasmid was quantified directly in the final sample and indirectly in the first supernatant. Proper samples for the calibration curve were also prepared (from 0-1 pmol). Samples were loaded in an agarose gel 2% (w/V) with 3 µL of the nucleic acid intercalator GelRed 100X in 100mL of TBE 0.5X, and ran at 150V during 35 minutes. Plasmid could be observed and quantified because the GelRed emits fluorescence when it is intercalated into the DNA and illuminated with UV light. Gel reader GeneGenius

(Syngene) and a UV-transilluminator were used to take the pictures, which were analyzed with ImageJ, and Microsoft excel was used to make the histograms.

3.7. Cell culture and viability assays

VERO cells were cultured in culture flasks (TPP) in DMEM medium (Dubelcco's modified Eagle's medium, Lonza) completed with inactivated fetal bovine serum (10% v/v), 2mM of L-Glutamine, 100 units/mL of penicillin and 100 µg/mL of streptomycin. They were incubated at 37°C and 5% CO_2.

For viability assays, MTT (Invitrogen) method was performed, following the manufacturer instructions. Cells were cultured in ELISA plates (96 wells), with $5 \cdot 10^3$ cells per well, and 200 µL of DMEM medium in each one. After 24 hours, the medium was removed, and 200 µL of new media was added to the positive control (100% of viability), 200 µL of water to the negative control (0% of viability) and 200 µL of different solutions of AuNPs diluted in DMEM (the content was never higher than 10%) to the other wells. All of the experiments were made in quintuplicate. They were incubated 24 hours at 37°C and 5% CO_2. Then, the medium was removed and 180 µL of new medium and 20 µL of MTT solution (3-(4,5-dimethylthiazol-2-yl)-2,5-diphenyltetrazol bromide, 5 mg/mL) previously filtered (with 0.2 µm filters) were added. Cells were incubated 4 hours at 37°C and 5% CO_2. Afterwards, the microplate was centrifuged for 30 minutes at 6000 rpm to make sure that the cells were fixed to the bottom of the well. The medium was removed and 100 µL of DMSO was used to solubilize the crystals produced in the cells. The absorbance of this solution was measured in a plate reader at a wavelength of 570 nm.

3.8. Cell transfection

For a preliminary screening, in a 96 well plate, 10^4 cells were seeded per well in 200 µL of DMEM medium without antibiotics. After 24 hours, wells were washed with PBS and 50 µL of transfection medium (DMEM without antibiotics or FBS with the appropiate transfecting agent and plasmid amount for each sample) was added.

The transfection agent used in the positive control was Lipofectamine™ 2000 (Invitrogen), added to the transfection medium and incubated for 5 minutes, and then mixed with the pEGFP plasmid in different concentrations (0.2-0.5; 0.6-1 and 1.2-1 pmol of pEGFP per µL of lipofectamine). The mixture was incubated for at least 20 minutes before been added to the cells. The transfection with nanoparticles was performed at two different concentrations: 0.1 pmol or 0.2 pmol of AuNPs previously incubated with 10-fold excess in pmol of plasmid were added in the same transfection medium.

Cells were incubated with the transfection medium for 4-6 hours, and then the media was removed and 200 µL of fresh DMEM medium with antibiotics and FBS were added. After 24 hours the transfection was evaluated in a fluorescence miscoscope. After 48 hours from the transfection, fluorescence microscope Eclipse Ti (Nikon) was used to take micrographs with the software NIS-Elements (Nikon).

In the final assay, a 24-well plate with coverslips at the bottom was used, and $5 \cdot 10^4$ cells per well were seeded. The procedure was performed as before, using 0.2 pmol of AuNPs previously incubated with a 10-fold excess in pmol of plasmid (2 pmol) and 0.4 pmol of plasmid with 1 µL of lipofectamine for positive controls in each well. Controls with 0.2 pmol of AuNPs without plasmid were also prepared. After 48 hours from transfection, cells were fixed and stained when necessary.

3.9. Cell fixation and staining

Cells have been previously grown over coverslips in a 24-well plate, as indicated the previous section. Medium was removed and wells were washed with DPBS (Lonza) 3 times. Then cells were fixed with 4% formaldehyde/PBS (Electron Microscopy Sciences) during 20 minutes at 4°C under agitation. They were washed again 3 times with DPBS, leaving the cells that would not be stained in that solution.

The first step for staining was adding permeabilising buffer (sucrose 0.3 M, NaCl 50 mM, $MgCl_2$ 6.3 mM, HEPES 20 mM and 0.5% Triton X in PBS pH 7.2) for 10 minutes at room temperature. After washing 3 times with DPBS, 1% BSA/PBS was added and incubated in the wells for 1 hour at room temperature. They were washed twice with DPBS. Then, anti-ß-tubulin IgG from mouse (Vector Laboratories) 1:50 solution in 1% BSA/PBS was incubated for 1 hour at 37°C. Cells were washed 3 times with PBS/0.5%

Tween and the secondary antibody anti-mouse from horse biotin-conjugated (Vector Laboratories) was added in a 1:100 solution in 1% BSA/PBS and incubated for 45 minutes at room temperature. Again, PBS/0.5% Tween was used for washing. Streptavidin-texas red (Atom, Vector Laboratories) from a 1 mg/mL stock was added in a 1:50 proportion in 1% BSA/PBS. Cells were washed then with DPBS 3 times. From a 5 mg/mL DAPI solution, a dilution 1:100 was added over the coverslips in PBS, and maintained for 10 minutes at room temperature. Then they were washed with DPBS and immersed on milliQ water before mounting them over a microscope slide, using ProLong Gold Anifade (Invitrogen). Finally, slides were kept protected from light overnight.

4. Results and discussion

4.1. Synthesis

AuNPs were synthesized by reduction of $HAuCl_4$ with sodium citrate. This method is quite simple and highly reproducible, and the proportion of citrate and gold precursor determines the size of the particles[22]. In this work, a molar ratio of 1:4.02 of chlorauric acid:citrate was used. The higher amount of citrate, the smaller the particles would be (it has been already discussed in the introduction that a high concentration of citrate prevents small particle from aggregation and forming bigger entities). TEM images were taken and AuNPs were measured, they have 13.43±1.12 nm of diameter.

The size of the AuNPs can be correlated to their UV-Vis absorbance spectrum[10], showing a maximum of the peak 519 nm. To identify aggregation, absorption spectrum is a useful tool, as interactions between AuNPs induce changes in the peak shape and maximum location, which is displaced to longer wavelengths.

However, the peak displacement is not only produced by aggregation; when some ligands are in contact with the gold surface, the dielectric constant changes and the peak may be slightly displaced too. The difference between aggregation and ligands effect is the length of the displacement and the observable change of the shape.

Absorbance spectra were used in this work to identify when nanoparticles aggregated or when their surface changed.

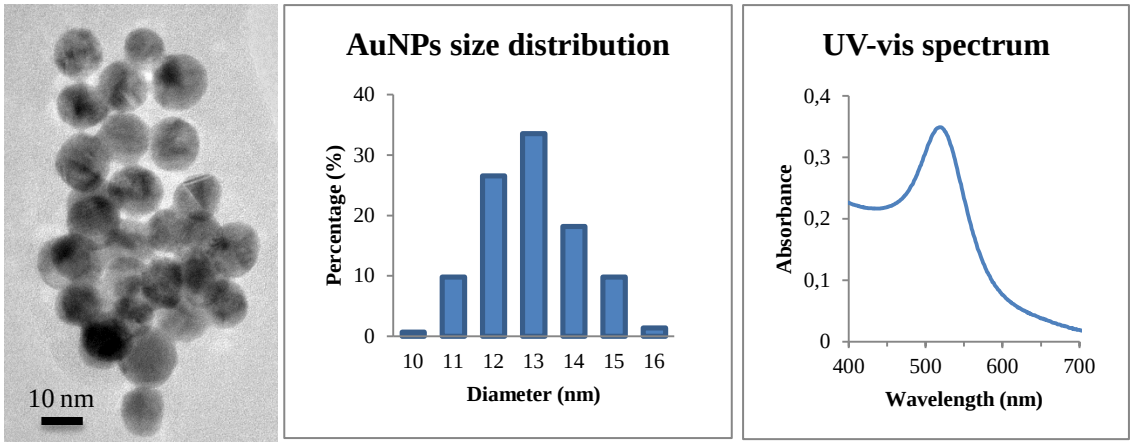

Figure 7: TEM image of the AuNPs, histogram with their size distribution and their spectrum of absorbance.

4.2. Functionalization

4.2.1. Stabilization

The next step consisted of providing the nanoparticles of a higher stability and at the same time adding functional groups that could be modified lately so as to attach a broad family of compounds for different applications.

The molecule used was PEG-COOH, which binds tightly by its thiol group to the gold atoms of the particle core, and has a carboxyl group on the other end that can be attached to other molecules. The polymeric nature of PEG provides a steric hindrance, producing repulsion between nanoparticles, which is strongly increased by the negative charges of the carboxyl groups. Additionally, it forms a coating that prevents adsorption of proteins and opsins[43,44], inhibiting for longer time the uptake by the reticulo-endothelial system and other clearance mechanisms, therefore allowing a more lasting circulation of the nanoparticles in biological systems.

Different quantities of PEG-COOH were incubated with the citrate-covered AuNPs in presence of SDS and NaOH. This assay provided information about differences in the coverage of the AuNP surface, and different covered nanoparticles were obtained to continue assays with the more appropriate ones. In addition, two protocols were compared: in one of them, nanoparticles were just incubated overnight at room temperature, and in the other, nanoparticles were sonicated for one hour before incubated overnight at room temperature again.

The histogram in Figure 9 compares the PEG-COOH chains attached to a nanoparticle. These data were obtained when applying Ellman's procedure to the washing supernatants. Those supernatants contained the excess of PEG-COOH molecules that did not react with the gold surface. The compound DNTB produces a colored complex in presence of thiol groups, and so, when added to the supernatants, the amount of color produced is proportional to the quantity of molecules with thiol groups. Those molecules can be quantified thanks to the color produced when reacting with DNTB (see figure 7). From the resulting thiol groups measured, PEG-COOH molecules that have been attached can be indirectly calculated.

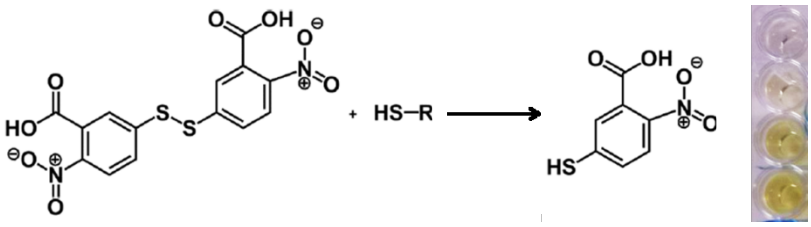

Figure 8: Reaction between DNTB and thiol groups. The obtained compound has a yellow color, with the same quantity of DNTB, the higher the number of thiol groups, the more intense the color is, as it can be observed in the picture on the right.

In figure 9, differences among the two incubation protocols can be observed. In every case, sonication produces higher PEG-COOH chains per nanoparticle ratio, except when 25 µg of PEG-COOH was added (but observing the mean error bar, the protocol could also produce a little higher ratio). The sonication protocol helps to increase a little the PEG-COOH ratio, probably due to the higher dispersion that it produces and that the sonication is likely helping to dissociate the citrate from the gold core and maybe even facilitating the approach of the thiol groups to that surface by keeping the PEG-COOH molecules extended.

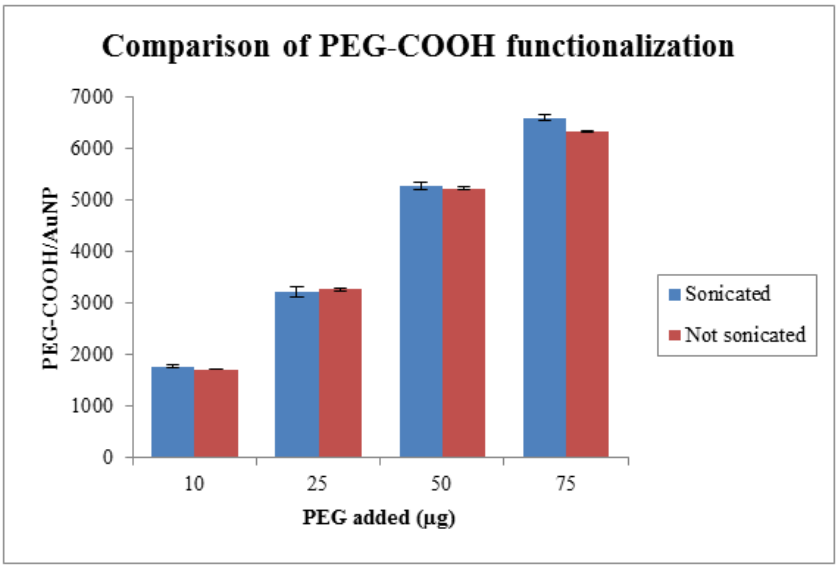

Figure 9: Histogram of the PEG-COOH chains calculated to be attached to one AuNP in two different conditions: sonicated before incubated overnight or just incubated overnight.

Two different conditions were chosen to continue with the functionalization: AuNPs were functionalized with the protocol without sonication and adding 25 µg of PEG-COOH per each 10 pmol of AuNPs (these are Au@COOH); AuNPs were also function-

alized using sonication with the biggest quantity (75 µg) of PEG-COOH per each 10 pmol of AuNPs (these are distinguished as sonicated Au@COOH).

These two different conditions were chosen to maximize the differences between the two kind of nanoparticles obtained, so they could be compared later on, when further functionalizations were done. However, due to the impossibility of testing the large number of types of nanoparticles that were produced, in DNA interaction assays, cell viability tests and transfection experiments only sonicated Au@COOH (after conjugation with adequate molecules) were used.

Though the number of PEG-COOH chains in the particle surface of both types of AuNPs was different, the Zeta Potential values obtained were quite similar. Data is shown in the next table.

Table I: Z-Potential of both types of Au@COOH

	Sonicated Au@COOH	**Non-sonicated Au@COOH**
Z-Potential (mV)	-21.1 ± 1.44	-19.8 ± 0.66

Once the nanoparticles were stabilized, the external carboxyl groups could be used for attaching different aminated molecules molecules through the EDC coupling reaction. When incubated with EDC and S-NHS, a reactive intermediate is formed, as it has been explained in the introduction, and amine groups can be attached to them, forming an amide group. In the next sections, activation conditions will be explained for each compound used in the conjugation.

Table II: Compounds conjugated to the AuNP surface and their main characteristics.

Molecule	Primary amine groups	Reason to be chosen	Advantages	Disadvantages
(2-aminoethyl)-trime-thylammonium	1	Permanent positive charge in quaternary ammonium group	The permanent charge can interact in any range of pH with negatively charged molecules as DNA	That permanent charge could bind too strongly the DNA to allow its release and expression inside the cell.
Tetra-ethylenpen-tamine	5	The different amine groups will have positive charges depending on their pKa and the pH of the solution.	Charges that change with the pH could be useful to release the DNA inside the cell.	To bind the molecule with-out producing crosslinking, different pH must be tested.
Ethylendiamine	2	The different amine groups will have positive charges depending on their pKa and the pH of the solution. Lower number of amine groups.	Charges that change with the pH could be useful to release the DNA inside the cell.	Just one amine group will be exposed on the surface, the charge varies depending on pH, interaction with DNA could be too weak.
Poly(ethyleneim ine)	Plenty	The different amine groups will have positive charges depending on their pKa and the pH of the solution. Higher number of amine groups.	Plenty of charges that change with the pH and that cover a higher volume could have a strong interac-tion with the DNA. Already used for gene transfection.	It is bigger than the other molecules and the high quantity of groups could produce NP crosslinking. The amount of positive charges could bond too strongly the DNA.
Tetramethyl-rhodamine 5-(and -6)-carboxamide cadaverine	1	Fluorescence. Easy conju-gation thanks to amine group.	-	-

4.2.2. (2-aminoethyl)-trimethylammonium as functional group

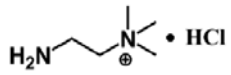

Figure 10: (2-ami-noethyl)-trimethy-lammonium hydro-cloridre.

(2-aminoethyl)-trimethylammonium ($R'R_3N^+$) is a molecule with a quaternary ammonium positively charged in all the pH range. On the other side of the molecule, it has an amine group, which can form an EDC and S-NHS mediated bond to carboxyl groups. Using this molecule to functionalize the AuNPs, permanent positive charges will be present in nanoparticle's surface, allowing strong ionic interactions with negative charged compounds as DNA. This kind of functionalization was tested before[39], producing AuNPs with positive Z potential that were unable to induce transfection. It was suggested that the high amount of charges could retain the plasmid with

the AuNP complex, and, in this project, the aim was functionalizing with less amount of $R'R_3N^+$ and conjugating also with TAMRA, to check nanoparticle's entrance to cells by fluorescence.

In the conjugation assays, electrophoresis in agarose 0.8% was used to check the retention of the samples. The electrophoretic mobility can be related to the net charge of the sample, and a complete retention in the well of the gel could be considered as a complete suppression of negative charges. This method is quick and simple; it provides information of the charge change in the AuNPs surface, though it is not quantitative.

Different quantities of EDC and S-NHS (always in 1:2 weight proportion) were used to activate nanoparticles for the conjugation with $R'R_3N^+$, and, even from the smallest amount (0.25 mg of EDC and 0.5 mg of S-NHS per 20 pmol of AuNPs), all the samples were retained in their wells when electrophoresis was performed. This was observed in both kinds of Au@COOH particles. The smallest quantity of EDC and S-NHS written above was used in further assays, as it already produced retention.

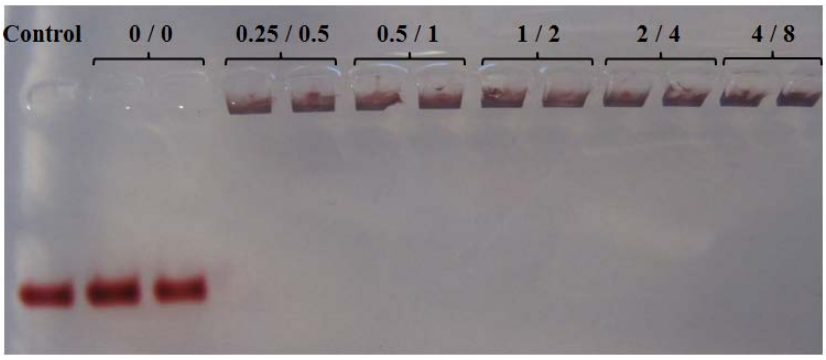

Figure 11: Photography of the agarose gel after the electrophoresis is developed. Different quantities of EDC and S-NHS (from 0 to 4 mg and from 0 to 8 mg, respectively, as it is written above the wells) were added in each kind of sample which was afterwards divided in duplicates. The same quantity of $R'R_3N^+$ was added in this case (2 mg per duplicate). When different quantities of $R'R_3N^+$ were added (from 0 to 2 mg per duplicate, and 0.25 mg of EDC and 0.5 mg of S-NHS were used) it could be observed the same result: all the samples were retained in the wells except those duplicates with 0 mg. These results were the same when sonicated and not-sonicated Au@COOH were used for the conjugation.

When different quantities of $R'R_3N^+$ were checked for the functionalization, every sample was retained in the agarose gel at the well level again. This was observed in both kinds of Au@COOH particles.

The following assays aim was to set the conditions to functionalize the AuNPs simultaneously with $R'R_3N^+$ and the fluorophore TAMRA. The fluorophore was added previously for avoiding interactions with $R'R_3N^+$ that could limit the reaction interfering with the activated carboxyl groups. One hour of incubation before adding $R'R_3N^+$ was sufficient to have differences (see figure 12) with the control (Au@COOH not activated). TAMRA was indirectly measured by quantifiying the fluorophore in the supernantans obtained after the washing steps.

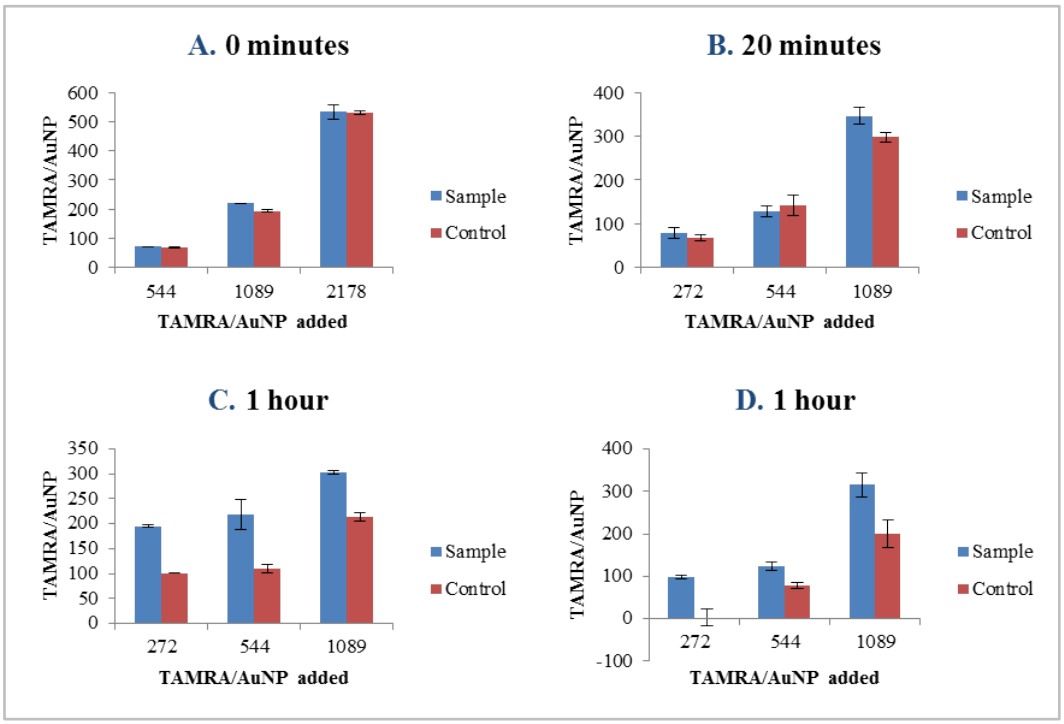

Figure 12: Histograms with the TAMRA per AuNP ratio at different times of incubation before adding $R'R_3N^+$. The difference between the samples is the TAMRA quantity added. Controls are AuNP in the same conditions but without activating with EDC and S-NHS their carboxyl groups. The mean error is calculated with two duplicates. Histograms (A), (B) and (C) are the results for non-sonicated Au@COOH; sonicated Au@COOH are represented in histogram (D). In (A) TAMRA quantity added was twice by mistake. As it can be observed, at short times (0 and 20 minutes) there was not enough difference between sample and control to consider that the TAMRA was being conjugated.

4.2.3. Tetraethylenepentamine as functional group

This molecule has five amine groups along its chain, by conjugating it to the nanoparti-

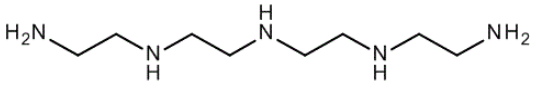

Figure 13: Tetraethylenepentamine structure.

cles, a surface that depends on pH to have positive charges was obtained.

This compound can induce AuNPs aggregation as it can react at the same time with carboxyl groups from different particles. That is why different pH conditions were checked in the first assay, as each amine group group has different pKa, and the amide bound is formed only when deprotonate amines are present, if many of them are protonated, crosslinking can be avoided. When the reaction with activated AuNPs was incubated at pH 6, aggregation and precipitation of particles were produced, but not at pH 7.5 nor at pH 9. At pH 9 the electrophoretic mobility was lower, probably because more groups could react, changing more the nanoparticle net charge, so that condition was used in following assays.

In this case, assays with different quantities of EDC and S-NHS and with different quantities of TEPA provided nanoparticles whose electrophoretic mobility was different between them. That can be observed in figure 14. There is a correlation between the quantity of the reactants added and the mobility in the gel. As it has a correlation with nanoparticle's charge, the more they move the more negative charges they have. That can be explained by the reactants quantity, the more there is the more can react, less free carboxyl groups would be present in the nanoparticle and more positive groups would be attached, therefore the net charge would be more positive and the mobility would be reduced.

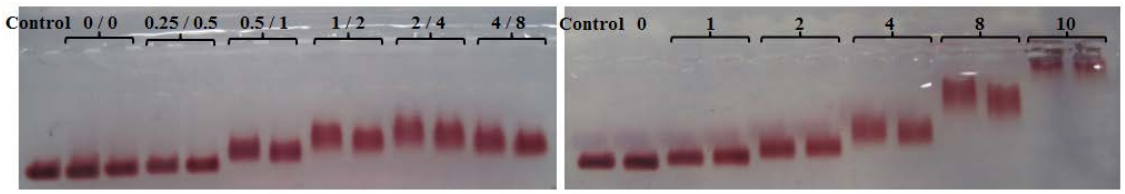

Figure 14: Images from agarose gel of samples functionalized with different quantities of EDC and S-NHS (left image) and different quantities of TEPA (image on the right) for sonicated Au@COOH. Quantities in mg are written over the wells for EDC / S-NHS per sample and in µL of a 1/100 solution for TEPA per duplicate. In A, TEPA quantity was 4 µL from a 1/100 solution. In B, AuNPs are activated with 0.5 mg of EDC and 1 mg of S-NHS. Similar results were obtained for not-sonicated Au@COOH.

These results provided the possibility of comparing the efficiency in transfection of different AuNPs as function of their surface net charge.

But, when performing assays of simultaneous conjugation with TAMRA and TEPA, nanoparticles were easily aggregated. Firstly, if TAMRA was added with the activated

AuNPs in pH 9, they were quickly precipitated. Somehow the mixture of TAMRA and activated AuNPs at pH 9 induced that effect (which was not produced at pH 6 or at pH 9 with non-activated AuNPs). As no fluorescence was observed in the washes, it is possible that the TAMRA reacted in a non-desired way with the carboxyl groups, producing at the same time nanoparticle precipitation and degradation of TAMRA. In figure 10 that effect can be observed.

Figure 15: Image of the sample conjugated with TAMRA at pH 9 after 45 minutes of incubation (left) and the non-activated control (right). AuNP precipitates are observed in the sample.

That was solved by adding the TAMRA and the activated AuNPs in a pH 6 MES buffer solution instead, and, after 45 minutes, centrifuging them, removing the supernatant and resuspending them in the pH 9 borate buffer for the incubation with TEPA.

The next problem to solve was AuNP aggregation during washing, as the high amount of salts present in PBS with tween 0.1% induced that effect. When nanoparticles were conjugated with a small amount of TEPA, they could be resuspended after a couple of washes with water, but if the amount of TEPA was slightly higher, they remained precipitated. That is the reason why only AuNPs with small amount of TEPA were simultaneously conjugated with TAMRA and used in further experiments.

4.2.4. Ethylendiamine as functional group

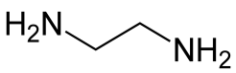

Figure 16: Ethylendiamine structure.

This diaminated molecule is also used to change surface charges. Incubation of the activated AuNPs with EDA was more effective in pH 6. The AuNPs had to be activated with 1 mg of EDC and 2 mg of S-NHS to maximize the differences between the functionalized AuNPs and the non-functionalized control, as EDA has only two amine groups (figure 16), and one is bonded to the carboxyl group in the AuNPs, instead of five as TEPA has (figure 13).

Different amounts of EDA were tested, and the highest was chosen to perform the next assays, as the difference with the control was very low for the rest of the samples.

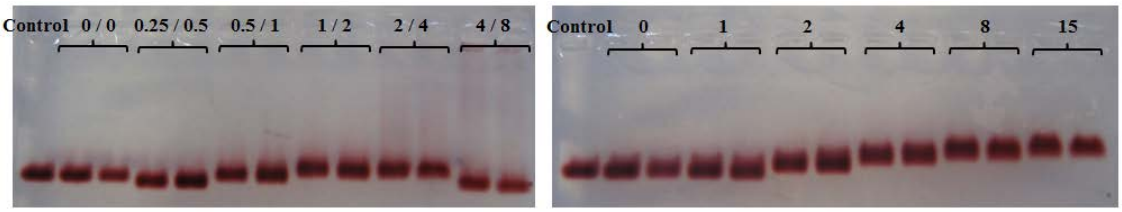

Figure 17: Pictures of electrophoresis in agarose gel show samples with different EDC / S-NHS amounts (in mg per sample, image on the left) and different EDA quantities (in µg per duplicate, image on the right). In the left image, 7 µg of EDA is added per duplicate, and in the right image the amount of EDC and S-NHS is 1 mg and 2 mg respectively. The retention produced by the surface change is smaller than for other compounds, but differences can be observed.

Simultaneous conjugation with TAMRA was also performed. No precipitation problems were observed while washing with PBS tween 0.1 %, suggesting that they are more stable than AuNPs with TEPA and TAMRA.

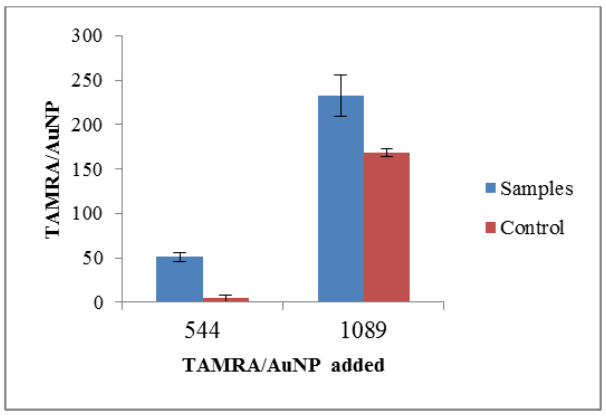

Figure 18: Histogram with the differences in TAMRA per AuNP ratio observed between activated sonicated Au@COOH and the same NPs but non-activated (control) when TAMRA is simultaneously conjugated with EDA. EDA was added 1 hour after adding TAMRA to the solution.

4.2.5. Poly(ethyleneimine) as functional group

Poly(ethyleneimine) (PEI) is a cationic polymer which has been already used in transfection and other delivery applications both alone[45] and in nanoscaled systems[46,47]. It can be purchased in many sizes and configurations.

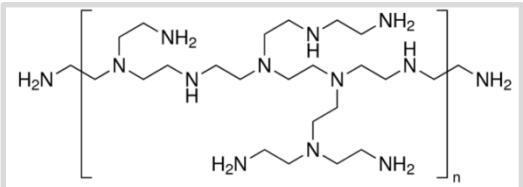

Figure 19: Structure of Poly(ethyleneimine).

Branched 25 kDa PEI is the most used for gene delivery and cell transfections, but it has showed a high cytotoxicity[47]. The one used in this work is represented in figure 18 and has an average molecular weight of 1300 Da.

This molecule has many amine groups that could interact with the nanoparticles, which means that AuNP aggregation could be easily produced. Activated AuNPs at different

pH were used in the first assay, to check the appropriate pH to have at least an amine group deprotonated, so it could react with the activated carboxyl group but not too many, to avoid many amines reacting and producing cross-linking between particles and therefore their precipitation. After 1 hour under agitation, nanoparticles at pH 7.5 and pH 9 were already precipitating, while AuNPs at pH 6 had experienced a color change but remained solubilized. When AuNPs were washed, as they were in duplicates, one was resuspended in water and the other in NaCl 1M to check the nature of the interaction (if it was just ionic, precipitated nanoparticles could be resuspended again when the amount of salts reduced those interactions). Only those at pH 6 could be resuspended, so the interaction between PEI and AuNPs was stable. In both duplicates, absorbance spectrum was measured, and a displacement of the peak was observed. The AuNPs in NaCl were clearly aggregated, but those on water did not have a great peak displacement. Moreover, the right side of the spectrum did not have high absorbance values, so there was no contribution from big aggregates.

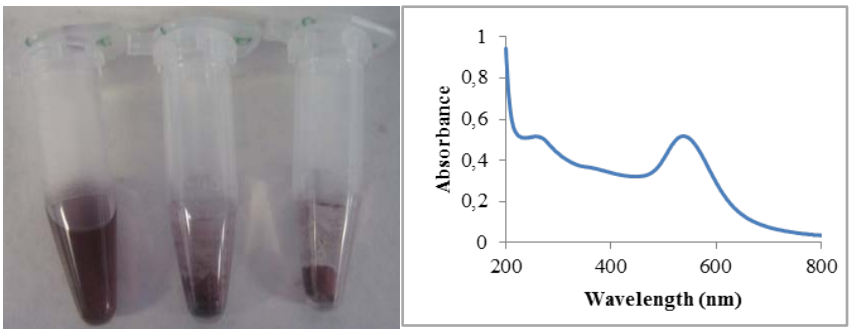

Figure 20: Picture of the AuNPs samples conjugated with PEI at different pH (those written over the microtubes) after the washing. On the right, absorption spectrum of those at pH 6, only them could be resuspended. The peak was displaced, but not as much as in aggregated AuNPs.

The color change produced in the solution and the displacement of the absorbance peak could mean that some aggregation is produced. Though the peak was more displaced than when it is just due to small changes in the surface (changes in dielectric constant), the shape of the spectrum was not very different from normal ones. When aggregation is produced, usually there is a greater absorption in the right side of the peak, due to contributions of bigger clusters of AuNPs. In this case, absorption in the right side of the peak remained similar to the observed when no aggregation is produced, so no big aggregates were formed. Somehow it could be a ‘controlled’ aggregation, where small AuNPs clusters were formed and remained stable in solution for some time.

Further experiments with different amounts of PEI showed that the higher the PEI quantity added, the less displacement of the peak of the functionalized AuNPs was observed. In addition, when PEI was added slowly and stirring, the sample had a greater color change and the peak in the absorbance spectra was more displaced, while when PEI was added quickly and mixing the sample immediately, the color change was not so great and the peak was less displaced. That may suggest that when AuNPs were quickly covered by a big amount of PEI, the interactions between two or more nanoparticles with the same PEI molecules could be less probable. PEI covering the whole AuNP would repulse another covered nanoparticle, while partially covered AuNPs could interact with the same PEI molecules, inducing aggregation. The first ionic interactions are probably decisive in the process, and they may guide how the covalent bond is produced.

Table III: Peak position in absorbance spectrum depending on the PEI amount

PEI/AuNP	$4.6 \cdot 10^3$	$4.6 \cdot 10^4$	$4.6 \cdot 10^5$	$4.6 \cdot 10^6$	$2.3 \cdot 10^7$	$4.6 \cdot 10^7$	$7.7 \cdot 10^7$
Peak (nm)	521	Aggregated	538	532	527	526	526

Though quite stable particles could be produced by this process, they were less stable than those conjugated with other molecules, and after one or two weeks they finally precipitated.

When functionalization was performed simultaneously with PEI and TAMRA, in the washing steps, the addition of PBS-tween 0.1% induced nanoparticle aggregation, but they were totally resuspended after two washes with water. Unfortunately, when they were in cell medium or any medium with relatively high amount of salts as TBE or PBS, particles aggregated and precipitated again.

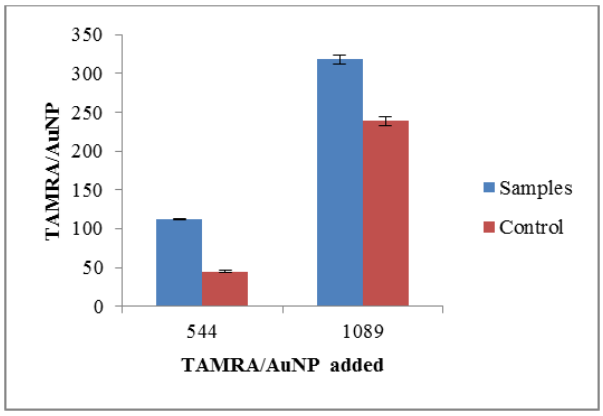

Figure 21: Histogram of the TAMRA per AuNP ratio, comparing activated sonicated Au@COOH reacting and non-activated controls. PEI was added after 1 hour of incubation with TAMRA. Similar results were obtained with non-sonicated Au@COOH.

4.2.6. Comparison between the different functionalizations

In the following table, main characteristics of the AuNPs are shown. The hydrodynamic diameter was measured by light scattering. Electrophoretic mobility percentage was calculated by comparing the displacement from the wells of the control and the sample, being 100% the displacement of the control and 0% was considered when the sample remained in the well. The distance was measured from the middle of the well to the middle of the electrophoretic band.

They have differences in Z potential that can be correlated to their electrophoretic mobility.

The hydrodynamic diameter measured can be affected by the fluorescence or the absorbance that the sample presents.

Table IV: Main characteristics of selected AuNP types

	Au@R'R_3N^+@ TAMRA	Au@TEPA@ TAMRA	Au@EDA@ TAMRA	Au@PEI@ TAMRA
Hydrodinamic diameter (nm)	338.0 ± 10.40	28.10 ± 9.60	13.50 ± 0.78	551.9 ± 5.35
Z Potential (mV)	-1.66 ± 0.47	-18.1 ± 0.58	-21.0 ± 2.41	-11.5 ± 0.25
Electrophoretic mobility (%)	0	82	90	0*
Absorbance Peak (nm)	520	544	520	530
TAMRA/ AuNP	45.82 ± 16.85	79.22 ± 19.79	46.24 ± 9.06	67.67 ± 2.30

*Au@PEI@TAMRA aggregated inside the gel well.

4.3. Interaction between nanoparticles and DNA plasmid

As the nanoparticles were devised to carry a DNA plasmid, interactions with that plasmid had to be measured, so the quantity of DNA per nanoparticle could be determined.

For that purpose, different quantities of plasmid (pEGFP) were incubated with 0.1 pmol of the different AuNPs. DNA was quantified directly from the mixture and indirectly from the washes that were made. Both quantifications provided pEGFP/AuNP ratio, which is shown in the histograms in figure 22.

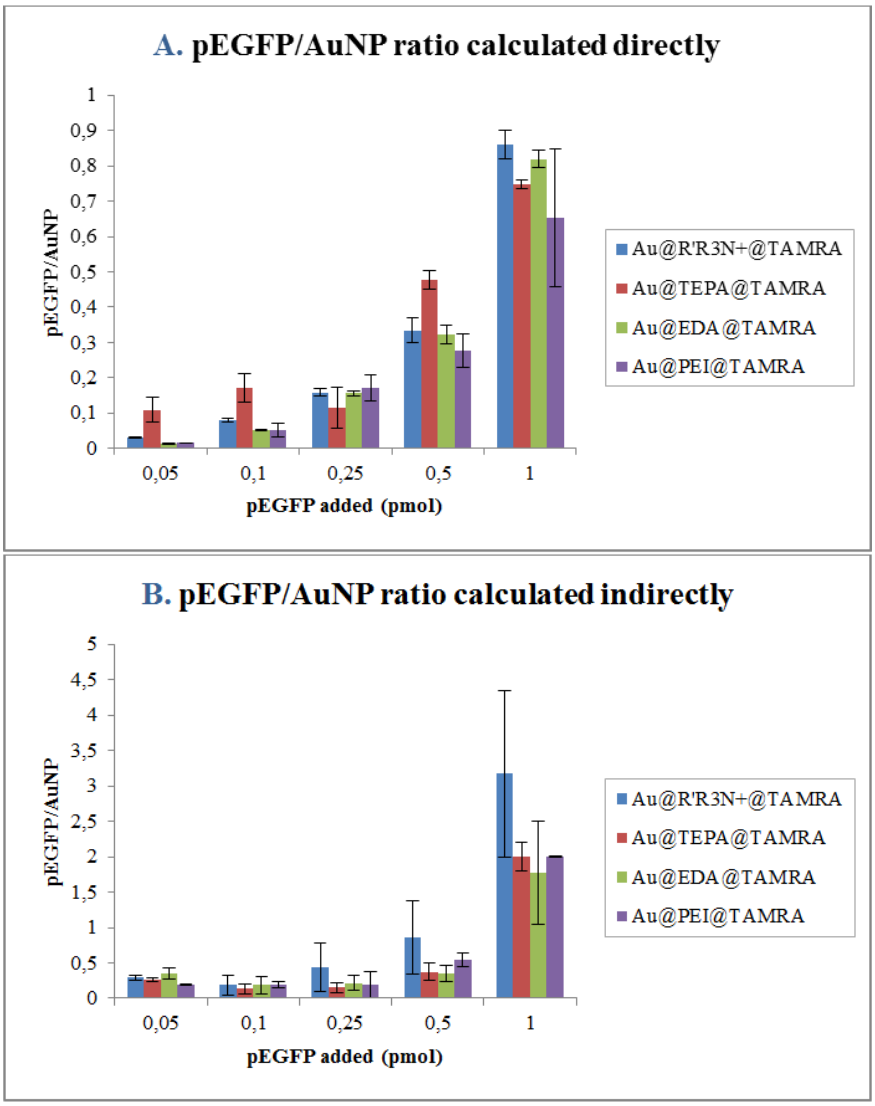

Figure 22: Histograms with the plasmid/nanoparticle ratio, calculed directly (A) and indirectly (B). Three different experiments in the same conditions are used to calculate the mean error, except for Au@PEI@TAMRA, which has only two different experiments.

Both results differed from each other, and pEGFP/AuNP ratio was bigger when it was measured indirectly and smaller when it is calculated directly. This difference may respond to the interactions between AuNP and the plasmid, which may interfere with the DNA intercalant dye (GelRed) –in the interaction between DNA and the intercalant or even by quenching effect in the fluorescence. These events would increase the difference, producing an underestimation in the direct calculus of pEGFP quantity.

Beside this, a precipitate was formed in every sample (although in samples with higher pEGFP/AuNP ratio this precipitate could be partially or entirely resuspended). It contained AuNPs because the color in the mixture that indicates presence of AuNPs faded

and in some cases even disappeared. In those samples where color disappeared pEGFP could not be detected in the electrophoresis, which means that the pellet also contained pEGFP. In samples with precipitate, as some plasmid could be lost in it, it would not be completely measured, therefore DNA calculated with the supernatants could be slightly overestimated. In any case, the mean error was quite high in every sample.

Indirect estimation was used to calculate the quantity of pEGFP/AuNP ratio when 1/0.1 pmol were used in the mixture (as it provided the higher ratio of pEGFP per AuNP in any of the cases, these quantities were chosen for the next experiments).

Table V: pEGFP/AuNP ratio for each AuNP type

	Au@R'R_3N^+@ TAMRA	Au@TEPA@ TAMRA	Au@EDA@ TAMRA	Au@PEI@ TAMRA
pEGFP/AuNP calculated indirectly	3.17 ± 1.18	2.00 ± 0.21	1.77 ± 0.73	2.00 ± 0.01

These results were a guide to calculate plasmid quantities used as positive controls in transfection assays.

Using electrophoresis in presence of GelRed has some limitations: the amount of DNA saturated the GelRed at the higher quantities, so maybe another technique could be more appropriate. DNA can be directly measured by spectrophotometry, but the amounts used might be too small to measure them by this way. Also direct measures of DNA and GelRed mixtures could be taken by fluorospectrofotometry.

4.4. Viability tests in Vero cells

Before applying the nanoparticles to their final purpose, the next step was evaluating the cell viability when exposed to AuNPs. Though AuNPs are biocompatible[7], changes in the surface would vary their properties, condition enough to increase nanoparticles' toxicity. As their possible toxicity would be more intense in presence of a higher amount of nanoparticles in the media, different concentrations of nanoparticles were used to test their effects over cell growth and survival through an MTT assay. This procedure uses the compound 3-(4,5-dimethylthiazol-2-yl)-2,5-diphenyltetrazolium bromide (MTT)to relate the number of living cells in the sample with the absorbance at 570 nm that can be measured at the end. When cells are active and viable, their mitochondria have

NAD(P)H-dependent oxidoreductase enzymes working, which can oxidize MTT to formazan, which is formed as insoluble crystals. Dissolving formazan in DMSO, the optical density of each sample can be measured, and with appropriate positive and negative controls, it can be related to the number of viable cells that are in the sample.

The protocol was applied with AuNPs conjugated to $R'R_3N^+$, TEPA and EDA (all of them simultaneously conjugated with TAMRA), and the results obtained are shown in figure 22 histogram. It is possible that some nanoparticles tightly attached to the cell surface or inside cells interfere with the absorbance measured, and that may explain why AuNPs with TEPA and EDA had higher viability percentage than the control.

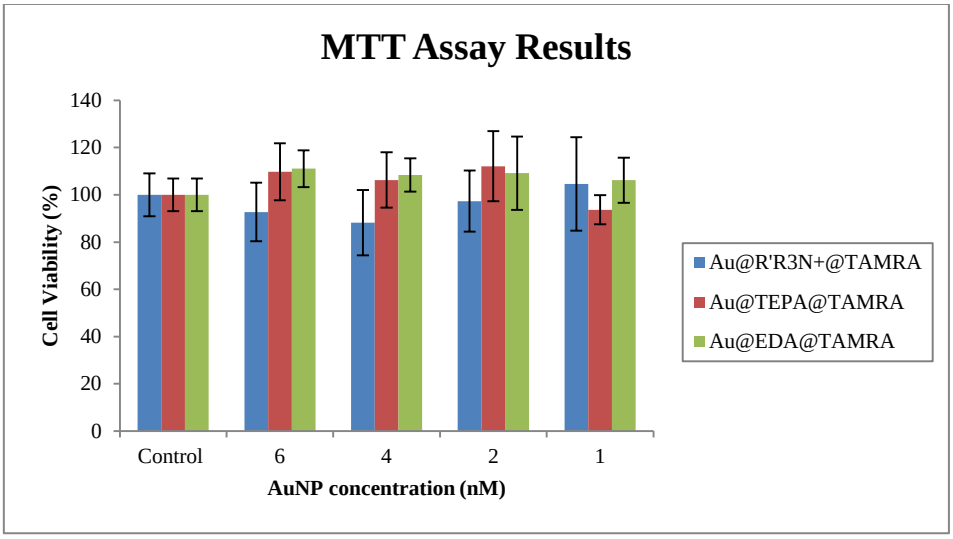

Figure 23: This histogram shows the data of the percentage of cell viability calculated by absorbance in a MTT assay. Cells are incubated in culture medium with different concentrations of AuNPs and the control does not have AuNPs but their volume in water.

Besides the error of this technique, some problems made impossible measuring cell viability with PEI functionalized AuNPs: they easily aggregated and precipitated in culture medium due to salt concentration, and AuNPs got attached to the bottom of the well. When measuring optical density, nanoparticles interfered, providing aberrant data. In one occasion, wells without cells were incubated with the AuNPs in culture medium to deduct their optical density from the one measured with the cells, but, as they did not have cells covering part of the surface, they precipitated even more, so the data was still aberrant.

Some other techniques could be used to measure cell viability, as long as the aggregated nanoparticles do not interfere with the measuring method. In this direction, the

LIVE/DEATH® kit (from Life Technologies) uses two fluorescent dyes that binds specifically to death or alive cells, allowing visual detection of both. This protocol does not require absorbance measures, however, AuNPs may have some quenching effect in the fluorophores, and the test could not provide the exact amount of death and alive cells. A simpler assay could be used instead: the membrane integrity of the cells can be checked using trypan blue, a dye that only enter in death cells. The main drawback is that it is much more time-consuming, as it requires counting all the cells, death and alive, present in the sample.

Due to the lack of time available, this technique was not implemented, but a check in the microscope allowed knowing if the cell morphology had changed and if the number of cells were visually fewer. In this case, such conditions were not observed; cells seemed unchanged compared to controls without nanoparticles (figure 24). This check did not provide quantitative data, just gives an approximate idea of how the cells were. In any case, aggregates could have influence in cell uptake of AuNPs.

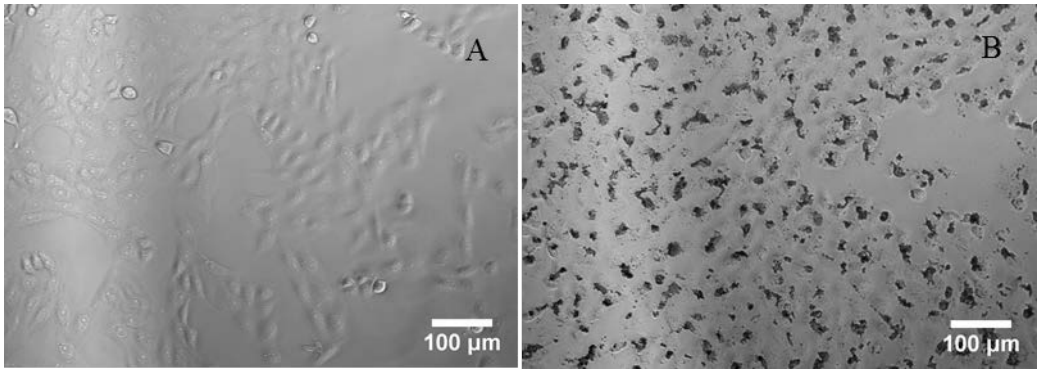

Figure 24: Cell pictures corresponding to (A) control cells and (B) cells incubated with 1 nM of Au@PEI@TAMRA for 24 hours. Big nanoparticle aggregates can be seen in (B).

Also, a viability test with AuNPs incubated with the plasmid was performed. Results are shown in figure 25. The viability is maintained in almost any case, except for Au@PEI@TAMRA, where could seem slightly reduced in the highest amount used. Anyway, it was not very significant, so these AuNPs did not induce a high cell death.

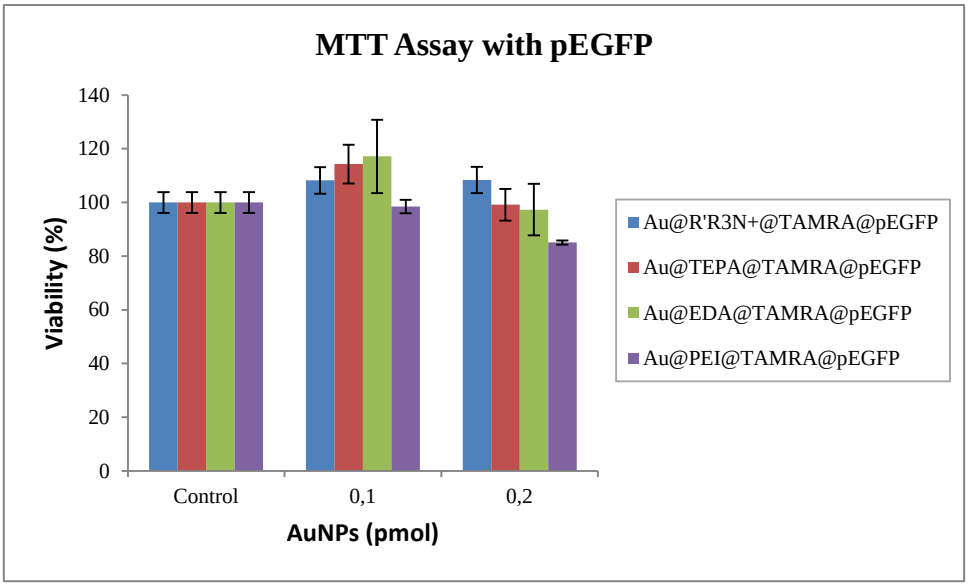

Figure 25: Histogram with the results of the viability assay performed with the AuNPs conjugated to the plasmid. Two amounts were added to the culture medium. Percentage was calculated with the absorbance measured.

4.5. Transfection assays in Vero cells

The transfection capability of these functionalized AuNPs was tested by conjugating ionically the DNA plasmid and incubating the cells with them for 6 hours in media lacking antibiotics and FBS. A positive control with Lipofectamine and DNA plasmid was performed simultaneously. Also, controls with AuNPs without plasmid were used to check if they reached and entered into the cells.

In those controls, TAMRA should have been useful to check cell internalization, however, AuNPs are probably producing a quenching effect. This is not produced when used with other metallic NPs, but AuNPs optical properties does. Some other techniques should be used to check cell internalization, such as TEM imaging of cell sections[19] or microscopy in dark field[48], which make possible detecting AuNPs in the cells. Due to the lack of time, these were not performed.

Cell samples treated with Lipofectamine showed morphology changes and high cell death but a great GFP expression. Lipofectamine has a great transfection capability, but also a toxic effect that produces cell death and changes in morphology.

On the contrary, none of the types of nanoparticles used induced such great changes in morphology. Cells were similar to those on the negative control, which means that their toxicity was quite low compared to Lipofectamine.

However, the GFP expression was much lower than the produced with Lipofectamine. In a first screening neither Au@R'R_3N^+@TAMRA nor Au@PEI@TAMRA produced fluorescent cells in the assay. Instead, Au@TEPA@TAMRA and Au@EDA@TAMRA did, but it was just a few cells in the entire well. In the final assay, when cells were fixed and dyed, some fluorescent cells were also found in all cases (Figure 26).

The fluorescence in some cells demonstrated that the nanoparticles were able to transfect a DNA plasmid inside the cells and allow its expression, which means that it was released from the AuNPs. The low amount of cells with EGFP found indicated that at some point of the transfection process the efficiency was not high enough. It could be possible that the charges in the AuNPs were not strong enough to retain the plasmid before entering the cell. On the other hand, AuNPs with the plasmid could not be entering into a big amount of cells, as they entered just by endocytosis and not by specific target. Finally, the problem could rely in releasing the plasmid inside the cells, if the interactions between AuNPs and the DNA were too strong.

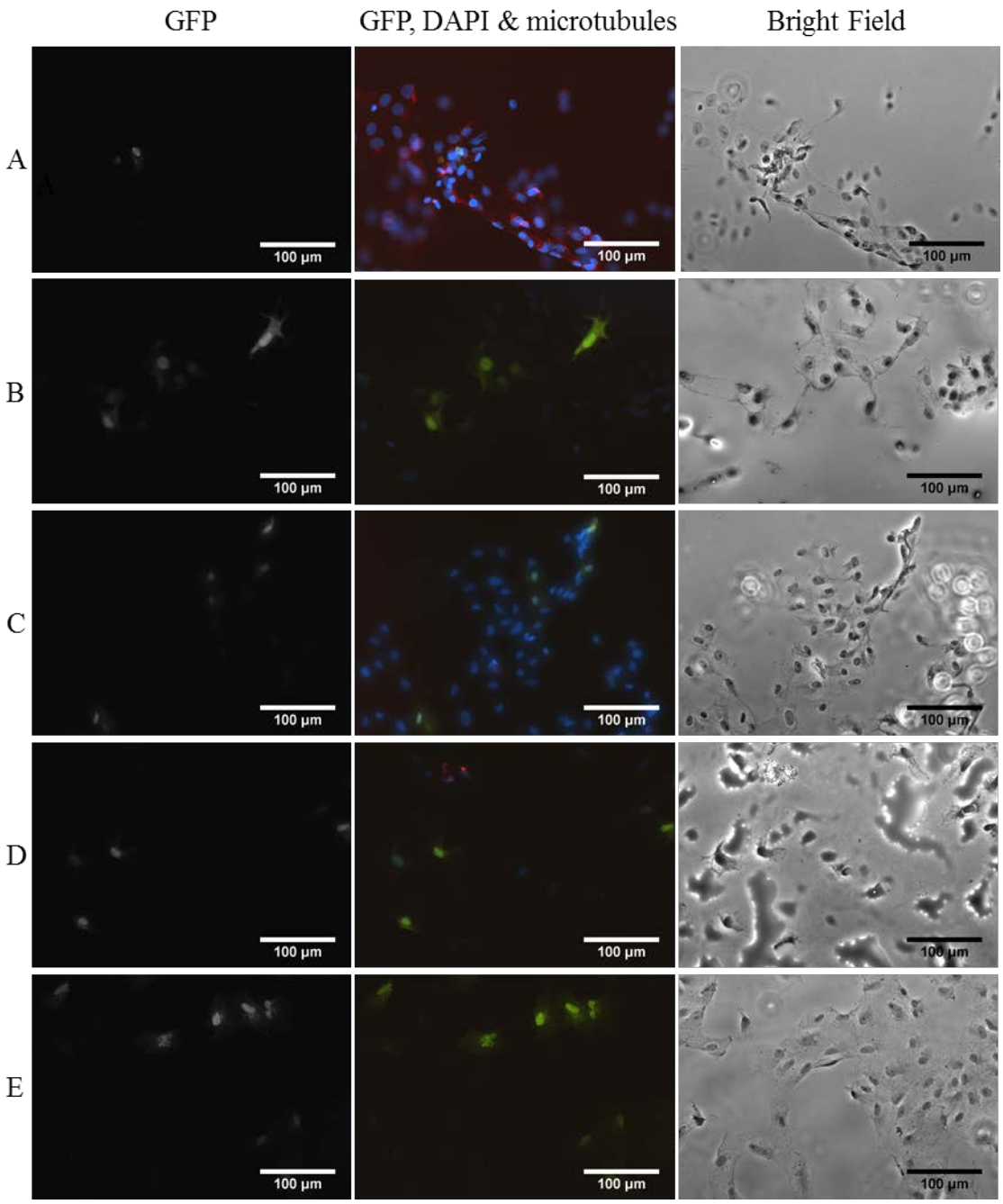

Figure 26: Images from fluorescence microscope of the transfected cells. In (A) cells were incubated with Au@R'R_3N^+@TAMRA, in (B) with Au@TEPA@TAMRA, in (C) with Au@EDA@TAMRA and in (D) with Au@PEI@TAMRA. The positive control is (E), and it was incubated with lipofectamine. GFP channel in grey scale is shown in the left images, GFP, DAPI and microtubule staining is shown in central pictures and bright field images are on the right. Microtubules were not well stained in some samples. Cell staining was not performed in control sample (E).

5. Conclusions and future perspectives

Along this work, differently functionalized AuNPs were produced with one type of cationic molecule and a fluorescent label. They were incubated with a DNA plasmid to check their interaction, to obtain appropriate vehicles for a transfection assay. Also, cell viability in presence of the AuNPs was tested.

During the functionalization, four types of AuNPs were selected and used in the next assays, one for each type of cationic molecule ($R'R_3N^+$, TEPA, EDA and PEI). The different molecules provided different characteristics to the nanoparticle surface, which could affect to the interaction with the DNA plasmid and to the cell viability.

During the optimization process of the functionalization many variants of the selected AuNPs were discarded, because not all of them could be tested in the available time. But maybe some of them could work better than the selected ones, so in future experiments, more types should be tested.

The ratio of plasmid ionically bonded to the nanoparticles was different when it was calculated directly or indirectly, so just indirectly measurements were considered to calculate plasmid amount attached to AuNPs in further assays.

The viability assays showed that 3 of the selected types of AuNPs were not cytotoxic, so they were suitable for working with biological systems. However, Au@PEI@TAMRA could not be tested with the MTT assay due to their aggregation and contribution in the absorbance measurements. Some other type of assay should be used to test properly the suitability of these nanoparticles for their use in biological systems.

Finally, the AuNPs were tested in transfection assays, where they induced EGFP expression in a few cells. Though they were working as transfection vehicles (some cells exhibited fluorescence), the efficiency is really low compared to the positive control. As they have advantages compared to Lipofectamine (this compound has high cytotoxicity, induces cell death and changes in morphology whereas AuNPs do not produce that effects), further optimizations of the nanoparticles should be assessed to increase the number of transfected cells. Maybe conjugation with a higher amount of cationic compounds could increase the conjugated plasmid, but if the strength of the bonding is too

high it may not be released inside the cells, so the equilibrium point should be found through more transfection tests.

Beside this, further test on cell internalizacion should be performed, such as TEM or dark field microscopy to discard AuNPs reach and entrance into the cells as the problem that affects the efficiency.

If these nanoparticles, once optimized their functionalization to have higher transfection efficiency, were used in more ambitious applications, like gene therapy, they would need some other molecules in their functionalization, such as peptides or carbohydrates, to target specific cells. In that way, not only they would transfect specifically the type of cell of interest, but also the transfection would be more efficient[45], because it would be more probable that AuNPs interacts with the cells thanks to targeting. All that would require further optimizations to increase the types of molecules attached without affecting to their stability. Beside this, *in vivo* assays would be required to test the behavior of these AuNPs in a complex biological system.

ACKNOWLEGEMENTS

I would like to thank the NAP group and the *Instituto de Nanociencia de Aragón* for the summer grant 'Introducción a la investigación 2014'.

Thanks to Jesús Martínez de la Fuente for the opportunity of working with the group. Thanks to Yulán Hernández, for her time and patience and for all the things she taught to me. Also thanks to Laura Asín, María Moros, Grazyna Stephen and Sara Rivera for helping me solving my doubts, and all the rest for their fellowship during the time I worked with them.

Thanks to Patty, Maron, Ana, Marta and Héctor Luis for their support during this time, and also to Javier and my parents, who were always there when I needed them.

Bibliography

1. European Commission. Enviroment. Deffinition of a Nanomaterial. *Enviroment* 1 (2014). at <http://ec.europa.eu/environment/chemicals/nanotech/faq/definition_en.htm>
2. Ramsden, J. *Nanotechnology. An introduction*. 288 (William Andrew, 2011).
3. NanoSpain. Catalogue of Nanoscience & Nanotechnology Companies in Spain. *Phantoms Found.* 88 (2013). at <http://issuu.com/phantoms_foundation/docs/catalogue_of_nanoscience___nanotech?e=3670244/4777199>
4. Mafune, F., Kohno, J., Takeda, Y. & Kondow, T. Formation of Gold Nanoparticles by Laser Ablation in Aqueous Solution of Surfactant. *J. Phys. Chem. B* **105,** 5114–5120 (2001).
5. Brust, M. & Kiely, C. J. Some recent advances in nanostructure preparation from gold and silver particles : a short topical review. *Colloids Surfaces A Physicochem. Eng. Asp.* **202,** 175–186 (2002).
6. Daniel, M.-C. & Astruc, D. Gold nanoparticles: assembly, supramolecular chemistry, quantum-size-related properties, and applications toward biology, catalysis, and nanotechnology. *Chem. Rev.* **104,** 293–346 (2004).
7. Shukla, R. *et al.* Biocompatibility of gold nanoparticles and their endocytotic fate inside the cellular compartment: a microscopic overview. *Langmuir* **21,** 10644–54 (2005).
8. Sperling, R. A., Rivera Gil, P., Zhang, F., Zanella, M. & Parak, W. J. Biological Applications of Gold Nanoparticles. *Chem. Soc. Rev.* **37,** 1896–1908 (2008).
9. Mie, G. Articles on the optical characteristics of turbid tubes, especially colloidal metal solutions. *Ann. Phys.* **25,** 377–445 (1908).
10. Haiss, W., Thanh, N. T. K., Aveyard, J. & Fernig, D. G. Determination of size and concentration of gold nanoparticles from UV-vis spectra. *Anal. Chem.* **79,** 4215–21 (2007).
11. Olofsson, L., Rindzevicius, T., Pfeiffer, I. & Ka, M. Surface-Based Gold-Nanoparticle Sensor for Specific and Quantitative DNA Hybridization Detection. *Langmuir* **19,** 10414–10419 (2003).
12. Faraday, M. The bakerian lecture: Experimental relations of gold (and other metals) to light. *Philos. Trans. R. Soc. London* **147,** 145–181 (1857).

13. Graham, T. Liquid Diffusion Applied to Analysis. *Philos. Trans. R. Soc. London* **151,** 183–224 (1861).

14. Yonezawa, T., Yasui, K. & Kimizuka, N. Controlled Formation of Smaller Gold Nanoparticles by the Use of Four-Chained Disulfide Stabilizer. *Langmuir* **17,** 271–273 (2001).

15. Rojo, J. *et al.* Gold glyconanoparticles as new tools in antiadhesive therapy. *Chembiochem* **5,** 291–7 (2004).

16. Huang, H. & Yang, X. Synthesis of Chitosan-Stabilized Gold Nanoparticles in the Absence/Presence of Tripolyphosphate. *Biomacromolecules* **5,** 2340–2346 (2004).

17. Schmid, G. *et al.* Au55[P(C6H5)3]12Cl6 - Ein Goldcluster ungewöhnlicher Größe. *Chem. Ber.* **114,** 3634–3642 (1981).

18. Brust, M., Walker, M., Bethell, D., Schiffrin, D. J. & Whyman, R. Synthesis of Thiol-derivatised Gold Nanoparticles in a Two-phase Liquid-Liquid System. *Chem. Commun.* 801–802 (1994).

19. Ojea-Jiménez, I., García-Fernández, L., Lorenzo, J. & Puntes, V. F. Facile preparation of cationic gold nanoparticle-bioconjugates for cell penetration and nuclear targeting. *ACS Nano* **6,** 7692–702 (2012).

20. Turkevich, J., Stevenson, P. C. & Hillier, J. A Study of the Nucleation and Growth Processes in the Synthesis of Colloidal Gold. *Discuss Faraday Soc* **11,** 55–75 (1951).

21. Frens, G. Controlled Nucleation for the Regulation of the Particle Size in Monodisperse Gold Suspensions. *Nat. Phys. Sci.* **241,** 20–22 (1973).

22. Kimling, J. *et al.* Turkevich method for gold nanoparticle synthesis revisited. *J. Phys. Chem. B* **110,** 15700–15707 (2006).

23. Lazarus, G. G., Revaprasadu, N., López-Viota, J. & Singh, M. The electrokinetic characterization of gold nanoparticles, functionalized with cationic functional groups, and its' interaction with DNA. *Colloids Surfaces B Biointerfaces* **121,** 425–31 (2014).

24. Ulman, A. Formation and Structure of Self-Assembled Monolayers. *Chem. Rev.* **96,** 1533–1554 (1996).

25. Brust, M., Fink, J., Bethell, D., Schiffrin, D. J. & Kiely, C. Synthesis and Reactions of Functionalised Gold Nanoparticles. *Chem. Commun.* 1655–1656 (1995).

26. Brennan, J. L. *et al.* Bionanoconjugation via Click Chemistry : The Creation of Functional Hybrids of Lipases and Gold Nanoparticles. *Bioconjug. Chem.* **17,** 1373–1375 (2006).

27. Nuß, S., Böttcher, H., Wurm, H. & Hallensleben, M. L. Gold Nanoparticles with Covalently Attached Polymer Chains. *Angew. Chemie Int. Ed.* **40,** 4016–4018 (2001).

28. Sztuka, K. & Kolodziejska, I. Edible films and surface coatings made of natural polymers for food packaging. Part II. Modifications. *Polymery* **53,** 725–729 (2008).

29. Rodrigues, R. C. *et al.* Amination of enzymes to improve biocatalyst performance: coupling genetic modification and physicochemical tools. *RSC Adv.* **4,** 38350 (2014).

30. Nakajima, N. & Ikada, Y. Mechanism of Amide Formation by Carbodiimide for Bioconjugation in Aqueous Media. *Bioconjug. Chem.* **6,** 123–130 (1995).

31. Bogdanov, A. A., Klibanov, A. L. & Torchilin, V. P. Protein immobilization on the surface of liposomes via carbodiimide activation in the presence of N-hydroxysulfosuccinimide. *FEBS Lett.* **231,** 381–384 (1988).

32. Sam, S. *et al.* Semiquantitative study of the EDC/NHS activation of acid terminal groups at modified porous silicon surfaces. *Langmuir* **26,** 809–14 (2010).

33. Liu, T. & Thierry, B. A Solution to the PEG Dilemma: Efficient Bioconjugation of Large Gold Nanoparticles for Biodiagnostic Applications using Mixed Layers. *Langmuir* **28,** 15634–15642 (2012).

34. Dreaden, E. C., Alkilany, A. M., Huang, X., Murphy, C. J. & El-Sayed, M. a. The golden age: gold nanoparticles for biomedicine. *Chem. Soc. Rev.* **41,** 2740–2779 (2012).

35. Collet, G., Grillon, C., Nadim, M. & Kieda, C. Trojan horse at cellular level for tumor gene therapies. *Gene* **525,** 208–16 (2013).

36. Ibraheem, D., Elaissari, a & Fessi, H. Gene therapy and DNA delivery systems. *Int. J. Pharm.* **459,** 70–83 (2014).

37. Dobson, J. Gene therapy progress and prospects: magnetic nanoparticle-based gene delivery. *Gene Ther.* **13,** 283–7 (2006).

38. Conde, J. *et al.* In vivo tumor targeting via nanoparticle-mediated therapeutic siRNA coupled to inflammatory response in lung cancer mouse models. *Biomaterials* **34,** 7744–53 (2013).

39. Hernández, Y. Funcionalización de nanopartículas de oro para terapia génica. 286 (2013).

40. Xun, M. *et al.* Low molecular weight PEI-based biodegradable lipopolymers as gene delivery vectors. *Org. Biomol. Chem.* **11,** 1242–1250 (2013).

41. Boussif, O. *et al.* A versatile vector for gene and oligonucleotide transfer into cells in culture and in vivo: Polyethylenimine. *PNAS* **92,** 7297–7301 (1995).

42. Haiss, W., Thanh, N. T. K., Aveyard, J. & Fernig, D. G. Determination of size and concentration of gold nanoparticles from UV-vis spectra. *Anal. Chem.* **79,** 4215–4221 (2007).

43. Harris, J. M. & Chess, R. B. Effect of pegylation on pharmaceuticals. *Nat. Rev. Drug Discov.* **2,** 214–221 (2003).

44. Ming, Z., Davidson, F. & Huang, X. Ethylene Glycol Monolayer Protected Nanoparticles for Eliminating Nonspecific Binding with Biological Molecules. *J. Am. Chem. Soc.* **125,** 7790–7791 (2003).

45. Sun, Y.-X. *et al.* The influence of RGD addition on the gene transfer characteristics of disulfide-containing polyethyleneimine/DNA complexes. *Biomaterials* **29,** 4356–4365 (2008).

46. Skandrani, N. *et al.* Lipid nanocapsules functionalized with polyethyleneimine for plasmid DNA and drug co-delivery and cell imaging. *Nanoscale* **6,** 7379–7390 (2014).

47. Hu, C., Peng, Q., Chen, F., Zhong, Z. & Zhuo, R. Low molecular weight polyethylenimine conjugated gold nanoparticles as efficient gene vectors. *Bioconjug. Chem.* **21,** 836–843 (2010).

48. Rosman, C. *et al.* A New Approach to Assess Gold Nanoparticle Uptake by Mammalian Cells: Combining Optical Dark-Field and Transmission Electron Microscopy. *Small* **8,** 3683–3690 (2012).